Aerosol and Air Quality Research

ORIGINAL RESEARCH
https://doi.org/10.4209/aaqr.220110

Geospatial Modelling for Estimation of $PM_{2.5}$ Concentrations in Two Megacities in Peninsular India

Special Issue:
Air Pollution and its Impact in South and Southeast Asia (III)

V.P. Lavanyaa [1,2], S. Varshini[1], Souvik Sankar Mitra[1], Kiran M. Hungund[1], Rudrodip Majumdar[1], R. Srikanth[1*]

[1] National Institute of Advanced Studies, Indian Institute of Science Campus, Bengaluru, Karnataka 560012, India
[2] Manipal Academy of Higher Education, Manipal, Karnataka 576104, India

ABSTRACT

Airborne particles finer than 2.5 microns ($PM_{2.5}$) constitute a major public health risk in India. Therefore, extensive scientific studies must be conducted to assess the $PM_{2.5}$ exposures of Indians and determine the "exposure-response function" specific to India. While Peninsular India includes three megacities with populations exceeding 10 million each, there are very few studies on air quality modelling in this region compared to North India. In this paper, the authors describe a Linear Mixed Effects (LME) model to estimate monthly-average $PM_{2.5}$ concentrations at a spatial resolution of 1 km^2 between 2016 and 2019 in the megacities of Bengaluru and Hyderabad with a total population of 23 million. This model is based on covariates such as aerosol optical depth (AOD), meteorological parameters, and Land-use-Land-cover (LULC) variables and is validated with extensive datasets from continuous and manual air quality monitoring stations through a 10-fold cross-validation process. The final LME model can explain more than 60 percent of the variation in the $PM_{2.5}$ concentrations in Bengaluru and Hyderabad. This model is then used to predict the monthly-average grid-wise $PM_{2.5}$ concentrations in more than 800 grids in each of these two cities to study the spatial and temporal patterns in $PM_{2.5}$ concentrations between 2016 and 2019. These spatiotemporal maps of $PM_{2.5}$ concentration are critical to overcoming the misclassification of exposure and will form a crucial input to much-needed PM exposure-response studies in these two megacities. This paper can serve as a useful framework for similar studies by showing the way to bridge the gaps in the current air quality monitoring network in Peninsular India.

Keywords: Aerosol Optical Depth (AOD), Linear Mixed Effects (LME) model, LULC classification, Exposure-response function, Spatiotemporal maps

OPEN ACCESS

Received: March 1, 2022
Revised: April 26, 2022
Accepted: May 5, 2022

[*] **Corresponding Authors**
rsrikanth@nias.res.in

Publisher:
Taiwan Association for Aerosol Research
ISSN: 1680-8584 print
ISSN: 2071-1409 online

1 INTRODUCTION

Fine particulate matter ($PM_{2.5}$) pollution is a primary global public health concern. It is the fourth global leading risk factor for premature mortality and accounts for 4.14 million deaths globally (Health Effects Institute, 2020). Several air pollution exposure studies in the last three decades suggest that prolonged exposure to $PM_{2.5}$ pollution is associated *inter alia* with respiratory and cardiovascular mortality and morbidity (Dockery *et al.*, 1993; Krewski *et al.*, 2005; Jerrett *et al.*, 2005, 2009; Pope *et al.*, 2002, 2009; Miller *et al.*, 2007; Samet *et al.*, 2000). However, the $PM_{2.5}$ attributable mortality burden varies sharply across countries based on their population, per capita income and levels of $PM_{2.5}$ exposure (Prabhakaran *et al.*, 2020). According to the Global Burden of Diseases (GBD) estimates, almost 58% of the global $PM_{2.5}$ attributable deaths occurred in Asia's two most populous countries, India and China which experience the highest $PM_{2.5}$ attributable age-standardized death rates of 89–98 per lakh population (Health Effects Institute, 2020).

ORIGINAL RESEARCH
https://doi.org/10.4209/aaqr.220110

Studies conducted during India's nationwide lockdown to control the spread of the COVID-19 pandemic have highlighted the reduction in the $PM_{2.5}$ concentrations in several Indian cities (Lavanyaa and Srikanth, 2020; Singh *et al.*, 2020; Mondal *et al.*, 2021). Beig *et al.* (2020) have studied the $PM_{2.5}$ concentrations measured in four megacities of India (Ahmedabad, Delhi, Mumbai, and Pune) during the unprecedented nationwide COVID-19-induced total lockdown starting from 25 March 2020. During the first fortnight of this lockdown, these four megacities in India were not impacted by any major external sources of air pollution. This rare combination of circumstances enabled these researchers to conclude that the baseline levels of $PM_{2.5}$ and other critical air pollutants in these four megacities exceed the WHO Air Quality Guideline (AQG) levels even though anthropogenic emissions were at a minimum due to the continued nationwide lockdown. In addition, Beig *et al.* (2020) have also quantified the increase in air pollutant concentrations due to external intrusions caused by changes in local meteorology in four cities (Ahmedabad, Delhi, Mumbai, and Pune). Therefore, the GBD-based exposure-response functions derived from cohort studies conducted in high-income countries with low ambient $PM_{2.5}$ concentrations are inapplicable to India (Prabhakaran *et al.*, 2020).

Human exposure assessment plays a vital role in epidemiological studies to estimate the long- and short-term health risks associated with $PM_{2.5}$ exposure. On the other hand, India has a sparse and non-uniform distribution of air quality monitoring stations (AQMS) even in urban areas and a near-absence of air pollution monitoring stations in rural areas (NGT, 2021; Prabhakaran *et al.*, 2020). Though, the Government of India launched the National Clean Air Program (NCAP) in non-attainment cities to reduce the ambient PM_{10} concentrations by 20 to 30% by 2024 compared to the corresponding levels in 2017 (MoEFCC, 2020a). The non-attainment cities are those cities whose PM_{10} concentration over the past five-year period exceeded the National Ambient Air Quality Standards (NAAQS). To monitor the ambient air quality in all non-attainment cities, the Central Pollution Control Board (CPCB) states that there is a need for 800 continuous AQMS and 1250 manual AQMS compared to the current availability of 193 continuous AQMS and 658 manual AQMS as of March 2021 (NGT, 2021). Therefore, as of March 2021, India has barely 50 percent of the number of AQMS needed to monitor air pollution only in the non-attainment cities, and most of the existing continuous AQMS are clustered in the National Capital Region (NCR) and the Indo-Gangetic Plain (IGP) (NGT, 2021). Further, while ambient air PM_{10} concentrations are monitored at 793 locations covering 344 cities, $PM_{2.5}$ is measured only at 274 locations covering 132 cities (MoEFCC, 2020a). Therefore, the use of $PM_{2.5}$ levels measured by a few AQMS as a surrogate for personal human exposure results in misclassification of exposure and causes bias in the exposure-response relationship (Monn, 2001; Özkaynak *et al.*, 2013; Shy *et al.*, 1978).

While the inadequate ground monitoring network creates a critical gap in air pollution-related epidemiological research in India, establishing such an air pollution monitoring network may be too expensive and time-consuming in a developing country like India. Over the past three decades, various methods such as GIS-based models, Land Use Regression (LUR) models, atmospheric dispersion models, and statistical models have been reported in the global literature to obtain robust air pollution exposure estimates. GIS-based models are heavily dependent on the density and distribution of AQMS (Beckerman *et al.*, 2012; Salam *et al.*, 2005; Jerrett *et al.*, 2005; Kim *et al.*, 2009). Therefore, several studies have used the chemical transport models to estimate the spatio-temporal $PM_{2.5}$ levels in India (Ojha *et al.*, 2020; Guttikunda *et al.*, 2019). LUR modelling is a widely used exposure estimation method successfully applied in different regions, including North America (Gilbert *et al.*, 2005; Ross *et al.*, 2006), United Kingdom (Stedman *et al.*, 1997; Briggs *et al.*, 2000) and India (Sanchez *et al.*, 2018). However, the LUR model captures only the spatial variation of the pollutant concentration and has limited application in estimating the Spatio-temporal variation of the $PM_{2.5}$ concentration. Several studies have used a statistical exposure modelling approach that utilizes the daily availability of satellite-derived Aerosol Optical Depth (AOD) at a high spatial resolution (1 km^2) with global coverage (Ali *et al.*, 2017; Sun *et al.*, 2017). AOD is a measure of columnar aerosol loading in the atmosphere based on the extinction of electromagnetic radiation and acts as a potential proxy for the ground particulate matter concentration (NOAA, 2012). Kloog *et al.* (2011) and Just *et al.* (2015) have used satellite-based AOD measurements and spatio-temporal covariates to model daily $PM_{2.5}$ concentrations in the Mid-Atlantic states and Mexico City using Linear Mixed Effects (LME) Model methodology. They showed that the model better performed than the other prevailing modelling approaches with

ORIGINAL RESEARCH
https://doi.org/10.4209/aaqr.220110

10- fold out-of-sample cross-validated (CV) R^2 of 0.81 and 0.724 in the Mid-Atlantic states and Mexico City, respectively. Maheshwarkar and Sunder Raman (2021) have shown that the spatial variability in the $PM_{2.5}$ concentration in Madhya Pradesh is reflected more accurately in the LME model than in the CTM based model of the same area. Several studies have used machine learning algorithms such as random forest, support vector machine, extreme gradient boosting, elastic net, and neural networks to improve prediction accuracy (Stafoggia *et al.*, 2017; Di *et al.*, 2016; Mandal *et al.*, 2020).

In this paper, the authors have used the LME model based on satellite-derived AOD, geographical and meteorological covariates to predict the monthly $PM_{2.5}$ concentration between January 2016 and December 2019 at a spatial resolution of 1 km^2 for the metropolitan regions of two cities in peninsular India—Bengaluru and Hyderabad. These cities have experienced rapid growth in land area as well as population during the last two decades due to the boom in the IT services sector in the last two decades. This boom has led to rapid increases in population, urban density, and number of vehicles. However, there are very few studies on the spatio-temporal changes in $PM_{2.5}$ concentrations in these two megacities of Peninsular India since most of the studies conducted in India are based on the National Capital Region and the Indo-Gangetic Plain.

The study period of this research was set as 2016 since this was the first full year during which ambient air $PM_{2.5}$ concentrations were first measured in these two megacities. The end of the study period was fixed as December 2019 to avoid the impacts of the unprecedented total lockdowns imposed in Bengaluru and Hyderabad for several weeks commencing 25 March 2020. Similarly, AQMS data recorded during 2021 are not considered since complete city-wide lockdowns to control the impacts of the 2nd wave of the COVID-19 pandemic were imposed in Bengaluru and Hyderabad starting in April and May 2021, respectively.

2 METHODS

2.1 Study Area

The geographical, climatological, demographic and topographical parameters related to the study areas in the megacities of Bengaluru and Hyderabad are shown in Table 1. The study areas include the respective municipal regions in Bengaluru (711 km^2) and Hyderabad (872 km^2). Based on the spatial orientation and shape of the land area within the respective municipal boundaries, the city of Bengaluru was divided into 801 grids (1 km × 1 km) matching with the spatial resolution of the Moderate Resolution Imaging Spectroradiometer (MODIS) - Multi-Angle Implementation of Atmospheric Correction (MAIAC) AOD, while Hyderabad was divided into 873 grids. The study areas in Bengaluru and Hyderabad are shown in Fig. 1.

Bengaluru and Hyderabad are located at different elevations (920 m and 545 m above Mean Sea Level, respectively). While Hyderabad remains warm throughout the year with maximum temperatures reaching 41 degrees centigrade, Bengaluru experiences moderate temperatures throughout the year with maximum temperatures limited to 34 degrees centigrade. In addition, Bengaluru experiences rain due to both southwest (SW) and northeast (NE) monsoons between June to September and October to November while Hyderabad receives most of the rainfall during the SW monsoon.

Bengaluru and Hyderabad have undergone rapid urbanization resulting in increased infrastructural activities and increased $PM_{2.5}$ pollution in the last couple of decades. However, the AQMS in Bengaluru and Hyderabad are primarily clustered in specific parts of the city. Therefore, attributing the $PM_{2.5}$ exposure measured at these stations to people residing far from the AQMS would result

Table 1. Key physical, geographical, and demographic information of Bengaluru and Hyderabad metropolitan areas.

City	Maximum Temperature (°C)	Minimum Temperature (°C)	Daily Average annual precipitation (mm)	Population (Million)			Decadal change	
				2000	2010	2020	2000–2010	2010–2020
Bengaluru	38	19	478.11	5.58	8.30	12.33	49%	48%
Hyderabad	41	20	1.37	5.65	7.53	10.04	33%	33%

Sources: IMD (2010–2020); Macrotrends (2022).

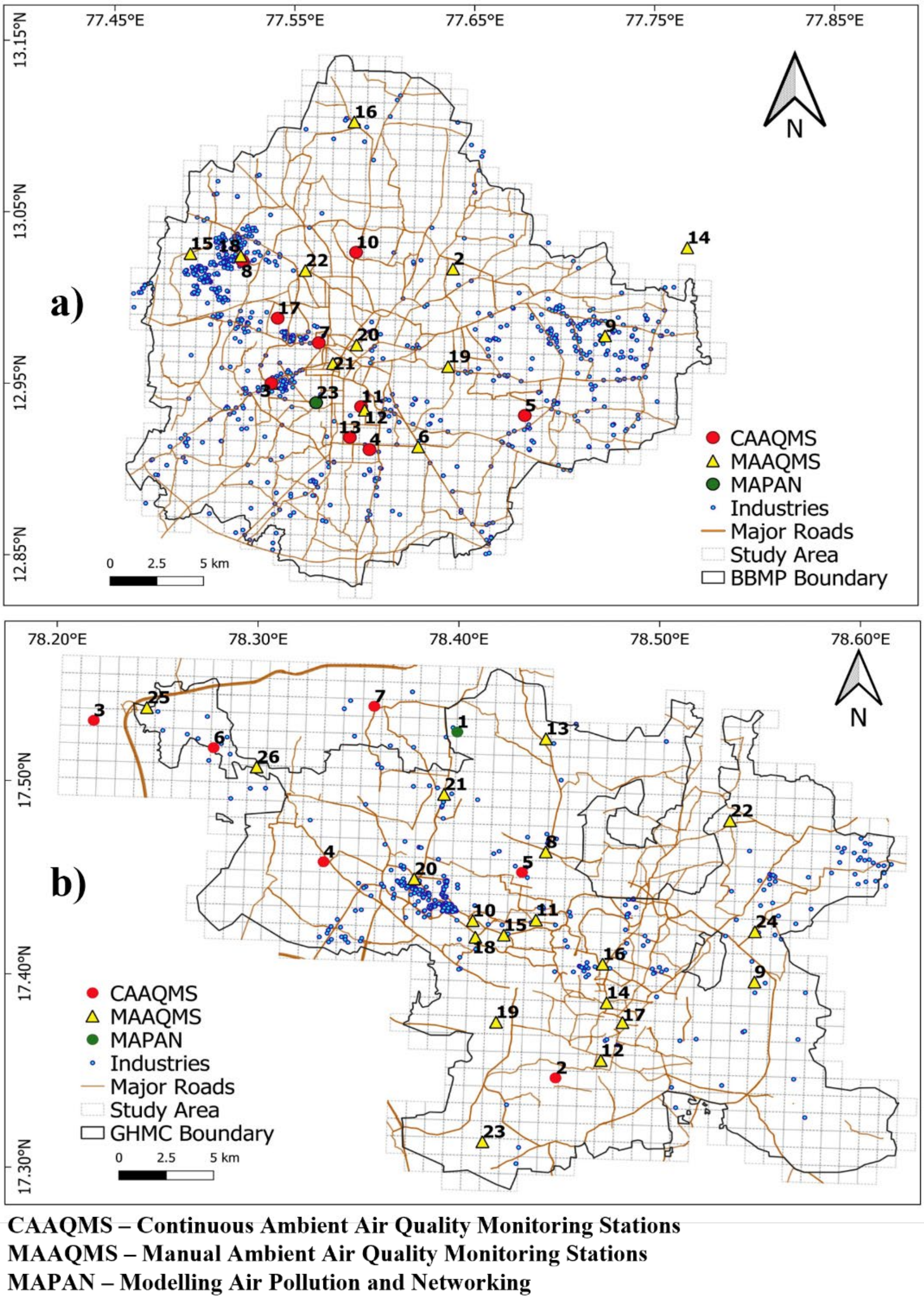

Fig. 1. Study areas in (a) Bengaluru and (b) Hyderabad.

in exposure misclassification. This anomaly poses several difficulties in relating the personal exposure of the people to mortality and morbidity statistics related to chronic and acute illnesses. Therefore, the dose-response relationship between the health impact and personal exposure can be better established in developing countries like India with the help of a high-resolution spatio-temporal $PM_{2.5}$ exposure model.

2.2 $PM_{2.5}$ Data

The ambient $PM_{2.5}$ concentrations used in this study were collated from both manual and continuous AQMS established and maintained by the Government agencies such as the Central Pollution Control Board (CPCB), the Karnataka State Pollution Control Board (KSPCB) in Bengaluru and the Telangana State Pollution Control Board (TSPCB) in Hyderabad between 2016 and 2019.

In addition, we have collated daily $PM_{2.5}$ concentration measurements from continuous AQMS established by the Indian Institute of Tropical Meteorology (IITM) under the Modelling Air Pollution and Networking (MAPAN) project. The continuous and manual AQMS installed by the CPCB, KSPCB, and TSPCB measure PM_{10} and $PM_{2.5}$ concentration based on beta ray attenuation and gravimetric method, respectively (CPCB, 2013). The MAPAN stations (one each in Bengaluru and Hyderabad) measure $PM_{2.5}$ using instruments calibrated based on U.S. EPA (Environmental Protection Agency) standards (Beig *et al.*, 2021). The minimum detection limit of the continuous AQMS instrument used at these AQMS is 2 $\mu g\ m^{-3}$. To ensure the quality of the collated daily $PM_{2.5}$ data, suitable data filters are applied during this study. $PM_{2.5}$ measurements below 10 $\mu g\ m^{-3}$ and not between $\mu^* \pm 3\sigma^*$ (*respective month-wise mean (μ) and standard deviation (σ)) were removed and considered missing (Mandal *et al.*, 2020). In addition, $PM_{2.5}$ measurements greater than PM_{10} measurements for co-located stations were removed and considered missing.

The monthly variability in the $PM_{2.5}$ concentrations recorded by continuous AQMS in Bengaluru and Hyderabad during the year 2019 is shown in Table 2. The $PM_{2.5}/PM_{10}$ ratio provides information regarding the source of emission of particulates. While the annual $PM_{2.5}/PM_{10}$ ratio in Bengaluru during 2019 varied between 0.36 and 0.52 in different AQM stations, this ratio varied in a narrow range (0.41–0.47) in Hyderabad. Therefore, the $PM_{2.5}$ and PM_{10} measurements in the co-located AQMS were used to predict $PM_{2.5}$ from PM_{10} measurements in Hyderabad, wherever $PM_{2.5}$

Table 2. Monthly average $PM_{2.5}$ concentration for all the real-time AQMS in Bengaluru and Hyderabad.

(a)	$PM_{2.5}$ ($\mu g\ m^{-3}$)	Jan	Feb	Mar	Apr	May	Jun	Jul	Aug	Sep	Oct	Nov	Dec	Annual Average
2016	Bapuji Nagar													
	BTM layout	66.9	67.8	61.8	56.4	47.5	23.6	17.5	12.5	17.0	33.2	22.1		44.4
	BWSSB Kadabesanahalli	59.5	52.4	30.8	42.6	36.6	17.8	19.5		27.1	34.7	44.7	22.2	39.6
	Hebbal													
	Hombegowda Nagar	Monitoring data is not available												
	Jayanagar													
	Peenya	75.9	89.8	85.4	40.2	33.2	29.2	21.3	25.6	37.9	61.2	53.4	49.0	52.8
	Silk Board													
2017	Bapuji Nagar	Monitoring data is not available												
	BTM layout	Monitoring data is not available										31.1		31.1
	BWSSB Kadabesanahalli	25.6	27.4	24.3	27.4	15.8	12.6	12.3	7.0	13.7	22.8	14.0	18.7	18.4
	Hebbal													
	Hombegowda Nagar	Monitoring data is not available												
	Jayanagar													
	Peenya	43.9	44.6	49.0	48.2	43.9	30.1	31.9	27.7	22.7	40.9	57.1	80.1	42.9
	Silk Board	Monitoring data is not available												
2018	Bapuji Nagar	Monitoring data is not available					19.2	21.8	26.3	31.3	41.7	48.6	59.3	38.0
	BTM layout	44.8	28.7	34.6	47.5	44.7	31.4	16.5	14.6	18.6	21.4	63.8	72.7	35.9
	BWSSB Kadabesanahalli	28.9	19.3	34.3	36.0	35.1	18.7	20.7	19.2	19.8	28.9	34.9	43.6	27.8
	Hebbal						9.0	13.3	11.6	19.2	32.3	40.0	58.0	24.0
	Hombegowda Nagar	Monitoring data is not available						13.3	11.9	18.8	32.5	35.4	47.7	26.7
	Jayanagar						14.0	15.4	13.5	21.0	59.6	52.4	67.1	36.6
	Peenya	50.0	42.6	37.4				25.6	25.0	32.6	39.3	32.8	43.8	36.0
	Silk Board	Monitoring data is not available					33.8	26.8	30.1	36.7	37.6	41.5	51.4	37.4
2019	Bapuji Nagar	59.6	48.6	46.0	42.2	45.8	35.7	27.5	21.5	21.1	28.9	45.6	34.1	38.0
	BTM layout	77.0	52.2	54.8	69.7	49.0	28.3	26.4	22.2	23.9	24.9	35.5	27.8	41.5
	BWSSB Kadabesanahalli	35.9	42.6	56.1	66.4	55.5	26.7	31.4	23.6	31.2	42.7	49.2	41.2	42.2
	Hebbal	59.6	47.0	42.2	39.7	32.4	16.3	11.6	9.5	15.9	22.8	40.1	38.2	31.2
	Hombegowda Nagar	49.2	40.7	40.8	34.7	30.9	15.4	12.0	10.9	9.9	11.2	35.4	29.8	27.3
	Jayanagar	59.2	45.8	42.1	35.7	30.6	16.0	9.7	9.9	17.0	27.8	45.3	37.2	31.2
	Peenya	47.3	42.2	65.4	62.9	37.8	31.5	28.3	20.2	21.8	21.9	26.2	38.1	37.4
	Silk Board	50.2	43.1	41.7	38.6	39.6	23.0	20.5	19.7	20.0	21.1	33.6	30.3	32.0

Table 2. *(continued).*

(b)	$PM_{2.5}$ (μg m^{-3})	Jan	Feb	Mar	Apr	May	Jun	Jul	Aug	Sep	Oct	Nov	Dec	Annual Average
2016	Bollaram	Monitoring data is not available									68.4	89.2	93.5	83.6
	Central University Hyderabad	49.5	40.2	41.3	33.3	21.1	15.5	10.0	10.7	15.4	57.2	76.6	73.5	36.7
	ICRISAT	Monitoring data is not available									49.6	94.3	87.0	76.7
	Pashamylaram	54.3	44.5	43.6	34.2	23.0	17.7	12.0	12.6	22.2	53.4	101.7	95.2	43.1
	Sanathnagar	108.9	77.7	60.8	53.8	51.1	46.7	44.3	10.4	18.7	44.6	73.0	86.7	55.2
	ZooPark	Monitoring data is not available												
2017	Bollaram	79.4	74.6	58.4	75.0	53.0	25.0	29.4	34.9	38.6	63.8	50.5	71.7	54.6
	Central University Hyderabad	66.7	60.8	44.6	47.5	30.8	11.1	13.0	13.4	18.9	40.7	46.9	69.8	38.6
	ICRISAT	71.8	64.6	48.5	56.1	33.5	9.6	12.5	16.3	23.3	47.9	53.8	72.6	42.4
	Pashamylaram	74.3	64.9	50.0	57.0	37.2	14.8	16.9	19.5	27.9	51.3	58.9	77.0	45.8
	Sanathnagar	81.6	91.7	54.0	61.8	44.1	23.2	20.7	25.7	33.9	64.5	61.9	103.3	55.4
	ZooPark	84.3	77.7	60.6	70.9	44.2	17.5	14.2	17.2	28.2	59.5	61.0	98.9	53.6
2018	Bollaram	74.7	53.2	62.6	43.7	39.3	27.5	22.3	26.7	42.6	63.0	53.7	67.4	48.0
	Central University Hyderabad	70.2	42.7	43.8	29.3	29.9	18.9	15.3	13.4	28.7	49.0	49.2	64.6	38.2
	ICRISAT	72.8	45.5	50.7	35.6	31.3	16.4	12.4	13.1	30.4	56.6	62.1	72.9	41.8
	Pashamylaram	81.3	48.2	51.9	35.5	34.3	19.5	13.3	13.9	32.9	61.8	69.7	79.4	45.4
	Sanathnagar	99.2	65.7	66.3	48.0	41.7	26.6	19.7	18.9	35.1	50.7	74.3	89.9	52.6
	ZooPark	96.0	57.6	56.6	37.2	35.5	22.7	19.5	21.2	50.6	76.8	76.9	95.5	54.4
2019	Bollaram	77.5	55.6	50.0	39.0	50.7	31.2	24.4	25.6	23.3	37.3	78.5	73.2	47.2
	Central University Hyderabad	69.5	47.3	38.5	30.0	36.4	15.8	8.9	9.3	13.9	27.7	60.2	53.4	34.1
	ICRISAT	74.6	52.1	40.3	31.0	37.4	16.9	14.4	15.8	18.8	36.2	73.1	65.6	39.7
	Pashamylaram	83.7	62.1	51.7	32.5	45.2	22.1	14.7	19.0	18.5	31.8	82.0	71.7	44.7
	Sanathnagar	93.0	61.0	51.2	41.7	45.3	29.4	21.5	19.9	24.8	53.3	85.2	82.1	50.7
	ZooPark	103.7	70.7	59.9	53.3	64.0	27.3	16.9	16.6	25.9	49.1	92.2	88.2	55.4

measurements were not available. In this case, the $PM_{2.5}$ levels are derived from the measured PM_{10} concentration using the LME model, with meteorological variables as covariates and month of the year as a random effect. The calibration model is cross-validated using the ten-fold cross-validation method (Stone, 1974). In the ten-fold cross-validation method, the entire dataset is randomly divided into ten equal parts, where the nine parts are used to train the calibration model, and the left-out part is used to test the model. The ten-fold CV R^2 of the $PM_{2.5}$ calibration model is 85.1% and the root mean squared error (RMSE) is 9.8 μg m^{-3} (Fig. 2; Table 3). This $PM_{2.5}$ calibration model is then used to predict the 9480 daily $PM_{2.5}$ values from PM_{10} measurements in AQMS across Hyderabad where $PM_{2.5}$ measurements are not available. In the next step, these

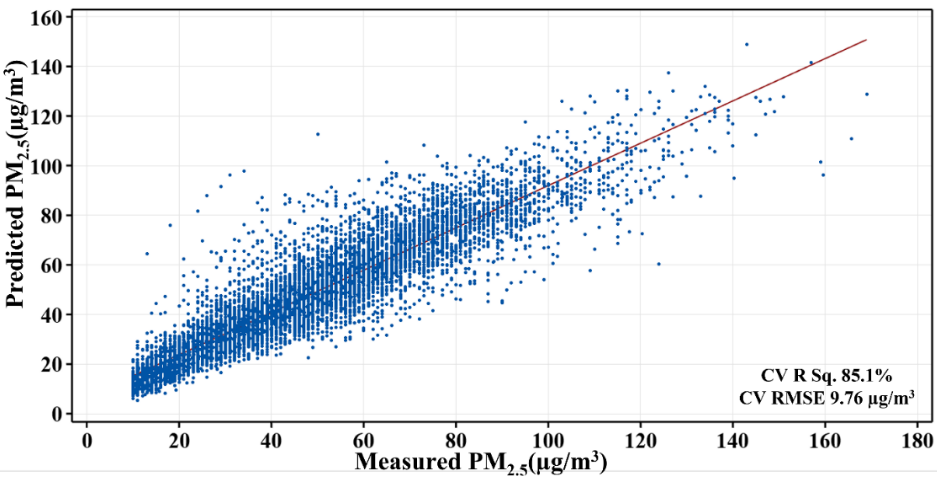

Fig. 2. 10-fold cross-validated $PM_{2.5}$ predictions from PM_{10} measurements in Hyderabad.

Table 3. $PM_{2.5}$ calibration model validation parameters in Hyderabad.

Year	MPE (μg m^{-3})	RMSE (μg m^{-3})	RPE (%)	10-fold CV R^2 (%)
2015	0.073	6.7	17.6	90.1
2016	0.013	9.3	19.4	89.1
2017	–0.014	11.0	21.7	81.6
2018	–0.031	9.5	20.1	83.2
2019	0.019	10.6	23.9	83.0
All	0.005	9.8	21.1	85.1

derived $PM_{2.5}$ values are added to the $PM_{2.5}$ measurements database that is used to build the final LME model. However, this method is not followed in Bengaluru due to the wide range of $PM_{2.5}/PM_{10}$ ratios between different stations. This variation in the $PM_{2.5}/PM_{10}$ ratio in Bengaluru is mainly due to the variability in the sources of emission around air pollution monitoring stations located in different areas that has also been documented in a study conducted by CSTEP (2022a) in this city. Consequently, the datasets of monthly $PM_{2.5}$ data used to develop the LME model had only 420 values in the case of Bengaluru and 1145 values in the case of Hyderabad.

2.3 Aerosol Optical Depth

MODIS is an instrument placed in the Terra and Aqua satellites launched by NASA that performs measurements in the visible to thermal infrared wavelengths. The local equatorial passing times of the Terra and Aqua satellites are 10.30 AM and 1.30 PM (Indian Standard Time), respectively. For this analysis, the daily MODIS AOD at 550 nm (AOD_{550}) data is derived using the MAIAC algorithm (Lyapustin *et al.*, 2018). The MAIAC algorithm is chosen since it has a relatively finer spatial resolution of 1 km^2 and better agrees with AERONET stations than other retrieval algorithms. However, the AOD_{550} observations over Bengaluru and Hyderabad are not continuous due to intermittent cloud cover, particularly during the monsoon season. In the case of Bengaluru, the AOD_{550} observations between July and October are almost completely absent. To impute missing entries in the MAIAC-AOD database, it is calibrated against the global atmospheric reanalysis based AOD from MERRA-2 (*Modern-Era Retrospective analysis for Research and Applications version* 2) using the Goddard Earth Observing System Model (GEOS) (Gelaro *et al.*, 2017). MERRA2 reanalysis data is available at a spatial resolution of 0.5° × 0.65° and 1-hour temporal frequency (Randles *et al.*, 2017). The gaps in the MODIS AOD are computed using the LME model with MERRA 2 AOD and geographical coordinates (latitude and longitude) of the centroids of the grids as covariates. The day of the year (DOY) is used as a random effect. The model is applied for every year between 2016 and 2019.

The year-wise R^2 and RMSE for the MAIAC AOD calibration models for Bengaluru and Hyderabad are given in Table 4. The year-wise linear models between the predicted and observed MAIAC AOD values are shown in Figs. 3(a) and 3(b) for Bengaluru and Hyderabad, respectively. As shown in Figs. 3(a) and 3(b), the MAIAC AOD calibration LME models performed well for all the four years between 2016 and 2019, for both Bengaluru and Hyderabad.

In this manner, the best-fit LME calibration models (one for each of the four years between 2016 and 2019) between the MAIAC AOD_{550} observations and MERRA2 reanalysis AOD_{550} data with the month of the year as random effect were used to fill the gaps in the AOD data. The daily predicted MAIAC AOD_{550} are then averaged on a monthly basis for incorporation into the final LME model.

Table 4. Year-wise MAIAC AOD_{550} calibration model results.

Year	Bengaluru		Hyderabad	
	RMSE	R^2 (%)	RMSE	R^2 (%)
2016	0.04	93.9	0.05	94.2
2017	0.04	93.6	0.04	89.4
2018	0.04	94.9	0.05	94.72
2019	0.04	93.3	0.05	89.6

(a)

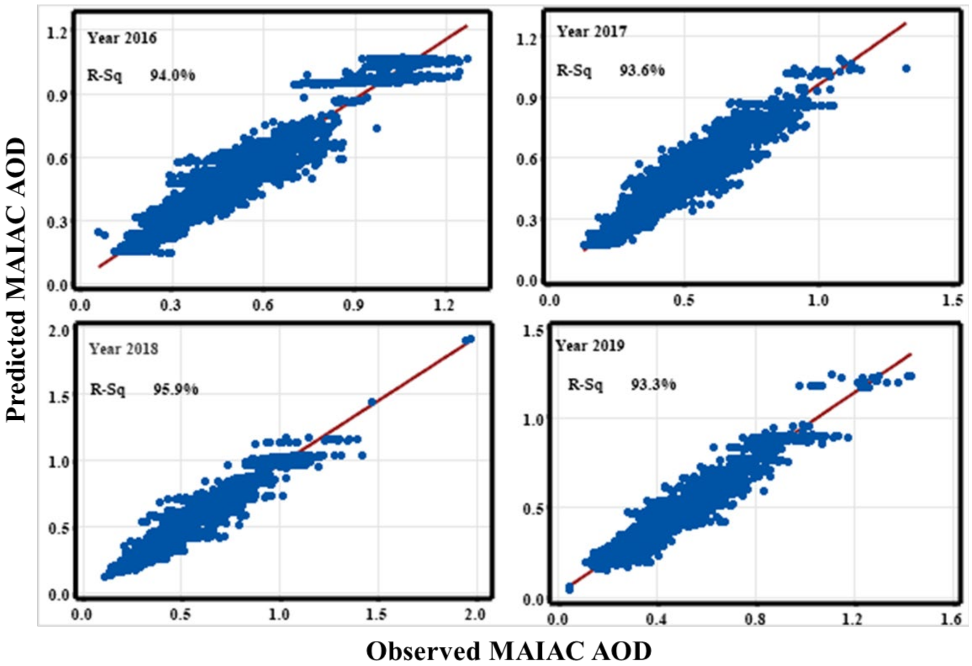

(b)

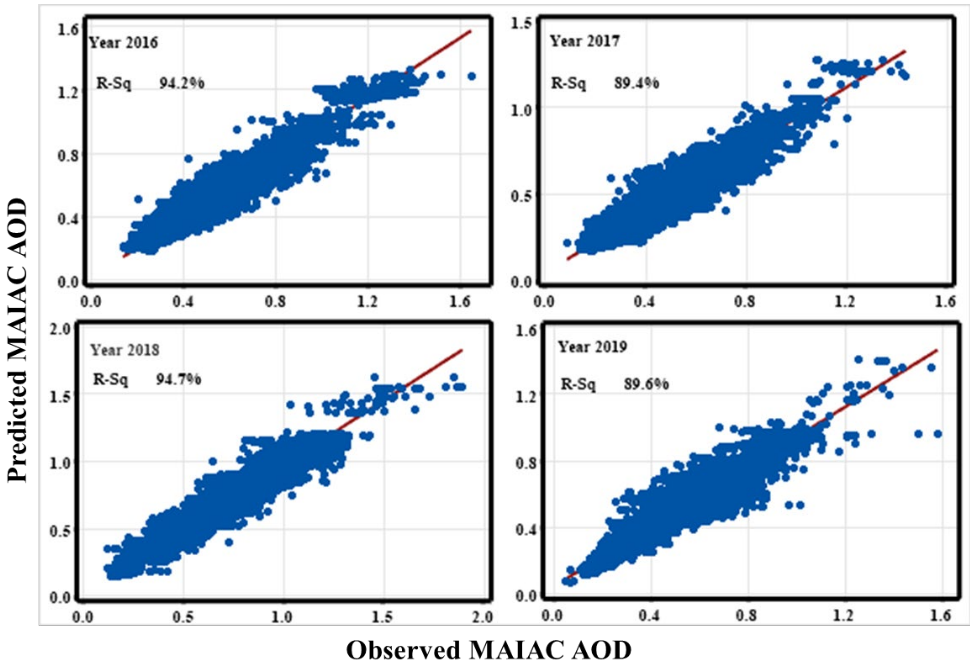

Fig. 3. Relationship between Predicted and Observed MAIAC AOD_{550} in (a) Bengaluru and (b) Hyderabad.

2.4 Geographical Covariates

2.4.1 Urban built-up

The impact of increasing built-up area on urban air pollution is well documented in the literature (Gaigne *et al.*, 2010). Therefore, the percentage of urban built-up area in each city is one of the critical predictor variables of the city's particulate pollution (Sarrat *et al.*, 2006). To extract the percentage of urban built-up within each 1 km × 1 km grid in the Bengaluru and Hyderabad study areas, two Landsat-8 (Collection 1) images in each year (one each from pre-and post-monsoon seasons) between 2014 and 2019 were downloaded from the U.S. Geological Survey (USGS) portal (https://earthexplorer.usgs.gov/). The bands 2–7 ((Blue, Green, Red, NIR, SWIR I, II) were stacked using the Q-GIS platform (QGIS Documentation, 2021). The stacked raster image was exported to the Google Earth Engine. The K-means clustering method was used to classify the image into 25 classes (Lloyd *et al.*, 1982). Further, the classified raster image was exported to the QGIS platform and compared with the original satellite image to get the different class numbers with similar spectral signatures.

In the case of Bengaluru, the classes with similar signatures were merged to form a combined class, leading to the classification of land use into four basic categories: urban built-up area, vegetated land, water bodies, and the barren land. However, in the case of Hyderabad, the merging of the similar signatures resulted in five final categories: urban built-up, vegetation, waterbody, fallow Land, and barren Land. It is noteworthy that the classified raster images of Hyderabad contained mixed pixels. Therefore, the reclassification of the raster image was done by overlaying the road network extracted from the Open Street maps portal (OpenStreetMap, 2021). While the satellite images of Hyderabad for 2015 and 2020 were classified using supervised classification in QGIS, the rest were classified using the K-means clustering method in the Google Earth Engine (Gorelick *et al.*, 2017). Figs. 4(a) and 4(b) show the LULC classified images of Bengaluru and

(a)

(b)

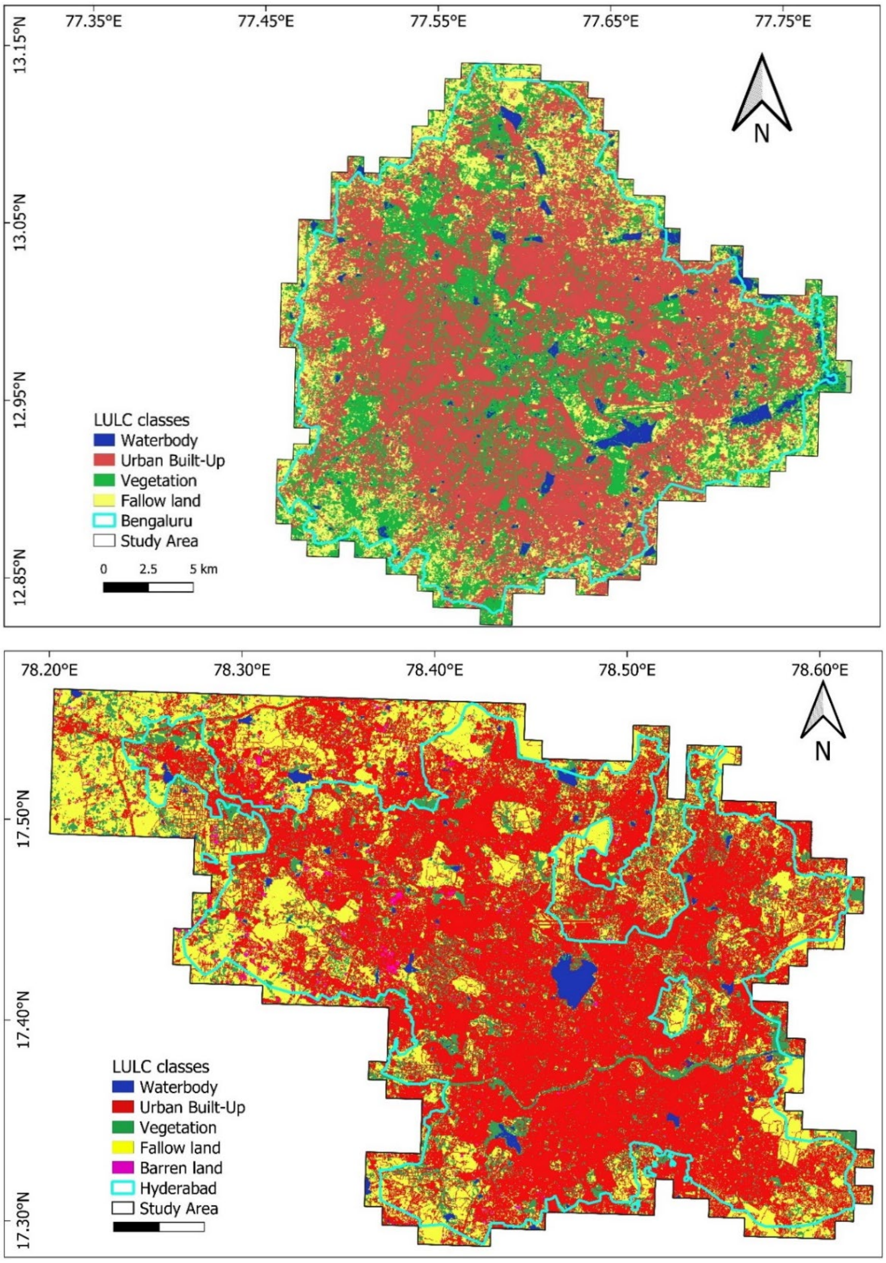

Fig. 4. Land Use Land Cover classified images of (a) Bengaluru and (b) Hyderabad in March 2019.

Hyderabad. Due to the 17% increase in the population of Bengaluru and a 12% increase in that of Hyderabad during the study period 2016–2019, Bengaluru and Hyderabad experienced increases in urban built-up areas of 12% and 11%, respectively (Macrotrends, 2022). The monthly increase in the built-up area in each grid is obtained by performing a cubic spline interpolation, assuming a gradual increase in the built-up area during the study period between 2015 and 2019.

2.4.2 Road density

The land use map for 2015 was obtained from the Bengaluru Developmental Authority (BDA), Karnataka, and the open street maps were used to extract the grid-wise road density in Bengaluru and Hyderabad respectively (BDA, 2015; OpenStreetMap, 2021). The road density is calculated as the sum of all the road lengths (primary, intermediary, tertiary) in the 1 km^2 grid divided by the grid area. The grid-wise road density was calculated using the QGIS platform (QGIS Documentation, 2021).

2.5 Meteorological Covariates

While the emission of pollutants is one of the key factors in the ambient concentrations of any pollutant, meteorological variables also interact with the pollutants via convection, advection, deposition, dispersion, and dilution. In this study, daily meteorological variables such as Temperature, Relative Humidity, Planetary Boundary Layer height, Surface Pressure, Wind Speed, and Wind direction are obtained from the Indian Monsoon Data Assimilation and Analysis (IMDAA) regional reanalysis data. This single-level IMDAA regional reanalysis data is maintained by the National Center for Medium-Range Weather Forecasting (NCMRWF) under the Ministry of Earth Sciences (MOES), Government of India (Rani *et al.*, 2021). This reanalysis data has a spatial resolution of 12 km and a temporal resolution of one hour (Rani *et al.*, 2021). Further, bilinear spatial interpolation was used on the daily IMDAA meteorological data files over Bengaluru and Hyderabad to obtain daily meteorological data at a spatial resolution of 1 km. The daily meteorological variables thus obtained were arithmetically averaged for each month. In the case of the planetary boundary layer (PBL) height, the monthly average of daily planetary boundary layer height between 6:00 AM and 6:00 PM IST is calculated. While the monthly wind speed was calculated using the scalar averages, the monthly wind direction was computed using vector averaging.

2.6 Model Development

As shown in Fig. 1, most of the AQMS in Bengaluru and Hyderabad are located near point or line emission sources. Since the $PM_{2.5}$ measurements at these AQMS exhibit a right-skewed distribution, the natural log transformation is applied to the response variable '$PM_{2.5}$' to ensure the homoscedasticity and normality of the residuals (Kloog *et al.*, 2011). Both geographical and meteorological variables are used in the model as covariates. Since the covariates that can enter, the model is screened using correlation and stepwise regression analysis, all the covariates considered for the model development are not included in the LME model. The correlations between $PM_{2.5}$ concentrations and AOD are statistically significant at the 95% confidence level in Bengaluru and Hyderabad with Pearson correlation coefficients of 0.315 and 0.349, respectively. The predictor variables such as temperature, relative humidity, wind speed, planetary boundary layer height, surface pressure, and road density correlate better with $PM_{2.5}$ measurements than any other predictor variables in Bengaluru and Hyderabad. Since several of the Spatio-temporal predictor variables used in the analysis have strong autocorrelation amongst themselves, including all the predictor variables in the model would result in a singular solution. Therefore, the predictor variables with the least autocorrelation are selected based on the stepwise regression method. The stepwise regression method is a statistical method that includes variables into the model until the R^2 value reaches saturation, after which there is no incremental change in the R^2 with the inclusion of any more predictor variables (Kutner *et al.*, 1983). Stepwise regression was performed between the log-transformed monthly average grid-wise $PM_{2.5}$ concentration (response variable) and the corresponding Spatio-temporal predictor variables between 2016 and 2019 in both Bengaluru and Hyderabad.

Several researchers have used each day of the study period as a random effect (Kloog *et al.*, 2011, 2014; Just *et al.*, 2015). However, a major part of the AQMS data in Bengaluru and

Hyderabad is derived from manual monitoring stations where the readings are not available for each day of the year. Therefore, we used each of the 48 months between 2016 and 2019 to assess the significance of this random effect. In the next step of the analysis, the LME model was applied with monthly-average $PM_{2.5}$ concentrations between 2016 and 2019 as the response variable and the predictor variables selected by the stepwise regression method in the previous step. The dummy months are assigned numerical values from 1 to 48 for the 48 months between January 2016 and December 2019 to assess the presence (or absence) of a month-specific random effect. The presence of a month-specific random effect indicates that the relationship between $PM_{2.5}$ and the predictor variables changes from month to month (Gałecki and Burzykowski, 2013). In this study, the parameter representing each of the 48 months between January 2016 and December 2019 was found to have a statistically significant random effect (p-values of 0.000 and 0.001 for the Bengaluru and Hyderabad datasets, respectively) on the $PM_{2.5}$ concentrations.

3 RESULTS AND DISCUSSION

3.1 LME Model Results and Discussion

The form of the final LME models relating the monthly-average $PM_{2.5}$ concentration and the selected geographical and meteorological covariates are shown in Eqs. (1) and (2).

Bengaluru

$$\log_e PM_{2.5(ij)} \sim (u_i + \beta_0) + \beta_1 AOD_j + \beta_2 RH_j + \beta_3 PBL_{ij} + \beta_4 SP_{ij} + \beta_5 Road\ density_j + \beta_6 Built-up_{ij} + e_{ij} \quad (1)$$

Hyderabad

$$\log_e PM_{2.5(ij)} \sim (u_i + \beta_0) + \beta_1 AOD_j + \beta_2 RH_j + \beta_3 WS_{ij} + \beta_4 PBL_{ij} + \beta_5 Built-up_{ij} + e_{ij} \quad (2)$$

$(u_i) \sim$ N $[(0, \sum)$
$e_{ij} \sim$ N $(0, \sigma)$

here, the $PM_{2.5(i,j)}$ is the $PM_{2.5}$ concentrations of the i^{th} month and j^{th} AQMS location. Similarly, the AOD_{ij}, RH_{ij}, PBL_{ij}, SP_{ij}, and WS_{ij} are Aerosol Optical Depth, Relative Humidity, Planetary Boundary Layer, Surface Pressure, Wind Speed, and Built-up area (%) on i^{th} month and j^{th} AQMS location. Road $density_j$ represents the road density at every j^{th} AQMS location. β_0 and u_i are the month specific fixed and random intercepts. $\sum$ denotes the variance covariance matrix of the random effect.

The final LME model coefficients are shown in Tables 5(a) and 5(b) for Bengaluru and Hyderabad, respectively. AOD, relative humidity, planetary boundary layer height and built-up area percentage

Table 5. Final LME model results.

Predictor variables	Coefficient	P-value
(a) Bengaluru		
Constant	33.842	0.000
Relative Humidity (%)	–0.051	0.000
Planetary Boundary Layer Height (km)	–1.094	0.003
Aerosol Optical Depth	0.731	0.020
Built-up Area (%)	0.970	0.000
Surface Pressure (kPa)	–0.285	0.000
Road Density (/km)	–0.012	0.000
(b) Hyderabad		
Constant	7.033	0.000
Wind Speed (m s^{-1})	–0.017	0.000
Built-up Area (%)	0.413	0.000
Relative Humidity (%)	–0.035	0.000
Planetary Boundary Layer Height (km)	–0.977	0.000
Aerosol Optical Depth	0.600	0.009

ORIGINAL RESEARCH
https://doi.org/10.4209/aaqr.220110

are the common covariates selected for both the Bengaluru and Hyderabad LME models. While surface pressure and road density are also having a highly significant impact (p-values of 0.000) on the monthly $PM_{2.5}$ concentrations in Bengaluru, wind speed has a highly significant impact in Hyderabad (p-value of 0.000). All covariates (except AOD) of the grid-level average $PM_{2.5}$ concentrations listed in Tables 5(a) and 5(b) are highly significant at the 99% confidence level, while AOD is statistically significant at 95% confidence level.

The ten-fold CV final LME model diagnostics for Bengaluru and Hyderabad are shown in Tables 6(a) and 6(b), respectively. The RMSE, Mean Prediction Error (MPE) and Relative Prediction Error (RPE) of the final LME model for Bengaluru were 8.39 µg m^{-3}, 6.4 µg m^{-3}, and 21.4%, respectively. The corresponding values in the case of Hyderabad are 11.3 µg m^{-3}, 8.2 µg m^{-3}, and 25%, respectively. The ten-fold CV R^2 values for Bengaluru and Hyderabad are 65.5% and 61.6%, respectively. The model validation parameters between the iterations of the 10-fold cross-validation procedure are consistent. The predicted versus measured values of $PM_{2.5}$ concentrations derived from the ten-fold CV LME models and the corresponding 95% confidence intervals are shown in Figs. 5(a) and 5(b) for Bengaluru and Hyderabad, respectively.

The cross-validated results of the model suggest that the final LME model can explain at least 60% of the variability in the monthly-average $PM_{2.5}$ concentrations in Bengaluru and Hyderabad. The grid-wise annual average $PM_{2.5}$ concentrations between 2016 and 2019 are predicted using the predictor variables belonging to the individual grid cells of the study area in Bengaluru (Fig. 6(a)) and Hyderabad (Fig. 6(b)). As shown in Fig. 6(a), hotspots of $PM_{2.5}$ concentration in Bengaluru are seen over the Peenya industrial area, the city railway station, the K.R. market, the Central Silk Board area, Whitefield, Hebbal, and Kalyan Nagar in all four years (2016–2019) irrespective of the seasons. Except for Peenya, the other hotspots are in areas witnessing dense traffic due to commercial activities. The south-eastern corners of Bengaluru have lesser $PM_{2.5}$ pollution for all the years between 2016 and 2019 due to the higher vegetation cover coupled with lack of commercial activities (Figs. 4(a) and 6(a)).

As shown in Table 2(a), the $PM_{2.5}$ pollution levels recorded in the continuous AQMS in Bengaluru peaked during the months between December and February. In the case of Hyderabad, the $PM_{2.5}$ pollution peaked between November and February (Table 2(b)). Though the $PM_{2.5}$ concentrations in most of the AQMS in Bengaluru comply with India's annual average National Ambient air Quality Standard (40 µg m^{-3}) for $PM_{2.5}$ concentration, the monthly average $PM_{2.5}$ levels during the winter months are much higher than the annual NAAQ standard (Table 2(a)). As expected, the $PM_{2.5}$ concentrations were low during the southwest monsoon period (June–September) in both Bengaluru and Hyderabad, and during the northeast monsoon period (October–November) in Bengaluru. Unlike Bengaluru, which experiences low $PM_{2.5}$ levels for six months between June and November, Hyderabad experiences low $PM_{2.5}$ levels only for four months (June–September) since the NE monsoon does not touch Hyderabad.

As shown in Fig. 6(b), the city of Hyderabad has hotspots of $PM_{2.5}$ pollution over the central parts

Table 6. Final LME model validation metrics.

Year	(a) Bengaluru (10-fold cross-validated)		
	MPE (µg m^{-3})	RMSE (µg m^{-3})	RPE (%)
2016	7.95	10.27	21.58
2017	4.93	6.53	16.19
2018	7.67	9.53	23.97
2019	5.71	7.29	22.21
All	6.45	8.40	21.41
Year	(b) Hyderabad (10-fold cross-validated)		
	MPE (µg m^{-3})	RMSE (µg m^{-3})	RPE (%)
2016	8.26	11.28	26.08
2017	8.57	11.22	23.40
2018	8.20	10.73	22.80
2019	8.00	12.01	28.22
All	8.25	11.31	25.02

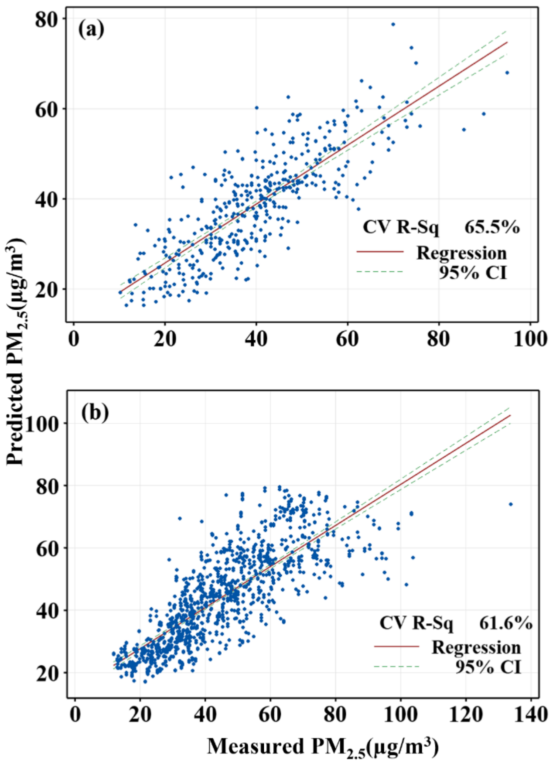

Fig. 5. Tenfold cross-validated $PM_{2.5}$ levels versus Measured $PM_{2.5}$ concentrations in (a) Bengaluru and (b) Hyderabad.

around Charminar, Paradise station, Jubilee Hills, and Jeedimetla. In contrast, the north-western parts of Hyderabad experienced comparatively lesser $PM_{2.5}$ concentration (25–30 µg m^{-3}) compared to other parts of Hyderabad (Fig. 6(b)). As shown in Table 2(b), the highest $PM_{2.5}$ levels in Hyderabad are recorded in the month of December compared to the corresponding values in other months.

While a sharp change in $PM_{2.5}$ concentrations is observable with change of seasons in Hyderabad, the monthly difference in $PM_{2.5}$ levels is low in Bengaluru, except during the change in season from monsoon to winter (Tables 2(a) and 2(b)). In Bengaluru, the $PM_{2.5}$ concentration declined between 2016 and 2019. This can be attributed to the major flyover and metro construction works that were taking place between 2012 and 2016 (Chaturvedi, 2012; Sastry, 2012; Mukherjee, 2012; The New Indian Express, 2017). The decline in the contribution of construction dust to the overall $PM_{2.5}$ concentrations in Bengaluru was also reported in two studies conducted by CSTEP firstly in 2015 and then in 2019 (CSTEP, 2022b; Guttikunda *et al.*, 2019).

The annual average $PM_{2.5}$ concentration in Bengaluru declined from 40.8 µg m^{-3} in 2018 to 33.2 µg m^{-3} in 2019. This sharp fall of 18.6% is also due to the steep fall of 36% in the annual average $PM_{2.5}$ concentration recorded in the Information Technology Park Ltd. (ITPL) in Whitefield after the closure of Graphite India Ltd from February 2019 pursuant to the order of the National Green Tribunal (The Hindu, 2019). Four other AQMS in Bengaluru also recorded a decline in annual average $PM_{2.5}$ concentrations ranging between 19% and 26% while some stations recorded a marginal increase.

In the case of Hyderabad, the $PM_{2.5}$ concentration were higher in 2016 and 2019 compared to 2017 and 2018. While other factors may also be at play, the impact of the steep reduction (75%) in the total precipitation in Hyderabad during 2017 (246 mm) compared to that recorded in 2016 (990 mm) is one of reasons for the average $PM_{2.5}$ concentration recorded in Hyderabad in 2017 being 10% higher than that in 2016 (IMD, 2010–2020). The increase in total precipitation from 246 mm in 2017 to 607 mm in 2018 and 682 mm in 2019 has played a major role in reducing the average $PM_{2.5}$ concentration in Hyderabad from 51.3 µg m^{-3} in 2017 to 48.8 µg m^{-3} and 42 µg m^{-3}, respectively (IMD, 2010–2020).

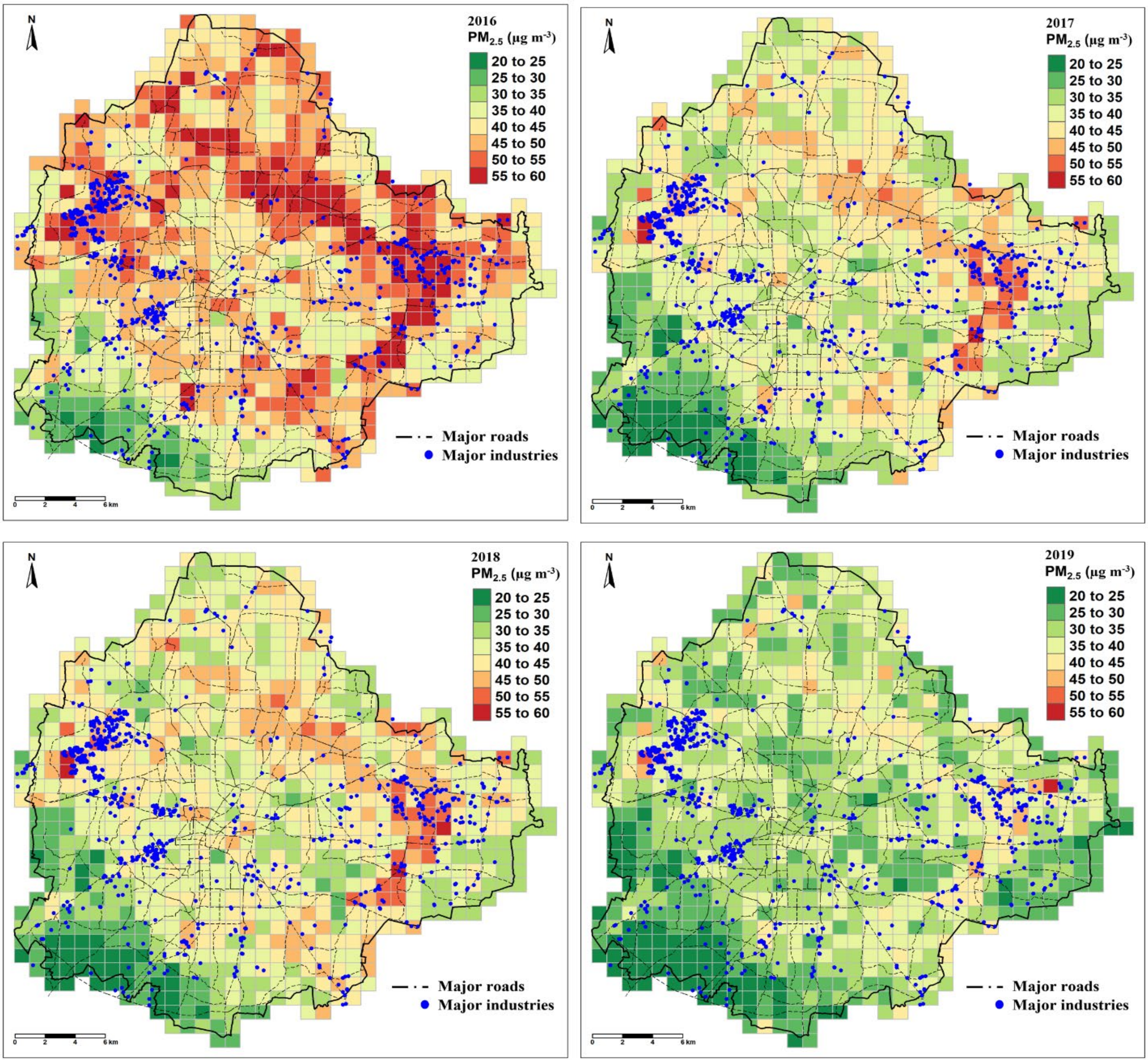

Fig. 6(a). Spatiotemporal distribution of model-derived annual average $PM_{2.5}$ concentrations in Bengaluru between 2016 and 2019.

All existing air pollution models in India use air quality data recorded by continuous AQMS only. Due to the paucity of continuous AQMS in Peninsular India even in the megacities, the ground-truthing carried out in earlier studies is inadequate to study the $PM_{2.5}$ pollution in the megacities of this region (Gupta *et al.*, 2020). As shown in Figs. 1(a) and 1(b), while the number of continuous AQMS in Bengaluru is more than in Hyderabad, $PM_{2.5}$ levels were not recorded in most of these stations in 2016 and 2017. However, continuous AQMS are expensive, costing more than Rs.30 million to procure and install per station (MoEFCC, 2020b). Therefore, the final LME models developed for Bengaluru and Hyderabad in the present study have used the $PM_{2.5}$ concentrations recorded in the manual AQMS as well as the continuous AQMS. The extensive datasets on PM pollution in the megacities of Bengaluru and Hyderabad collated from a wide variety of sources (CPCB, KSPCB, TSPCB, and IITM) to develop LME models to estimate monthly average $PM_{2.5}$ levels at a 1 km × 1 km grid level with a much higher level of performance compared to earlier studies is a major contribution of this study.

https://doi.org/10.4209/aaqr.220110

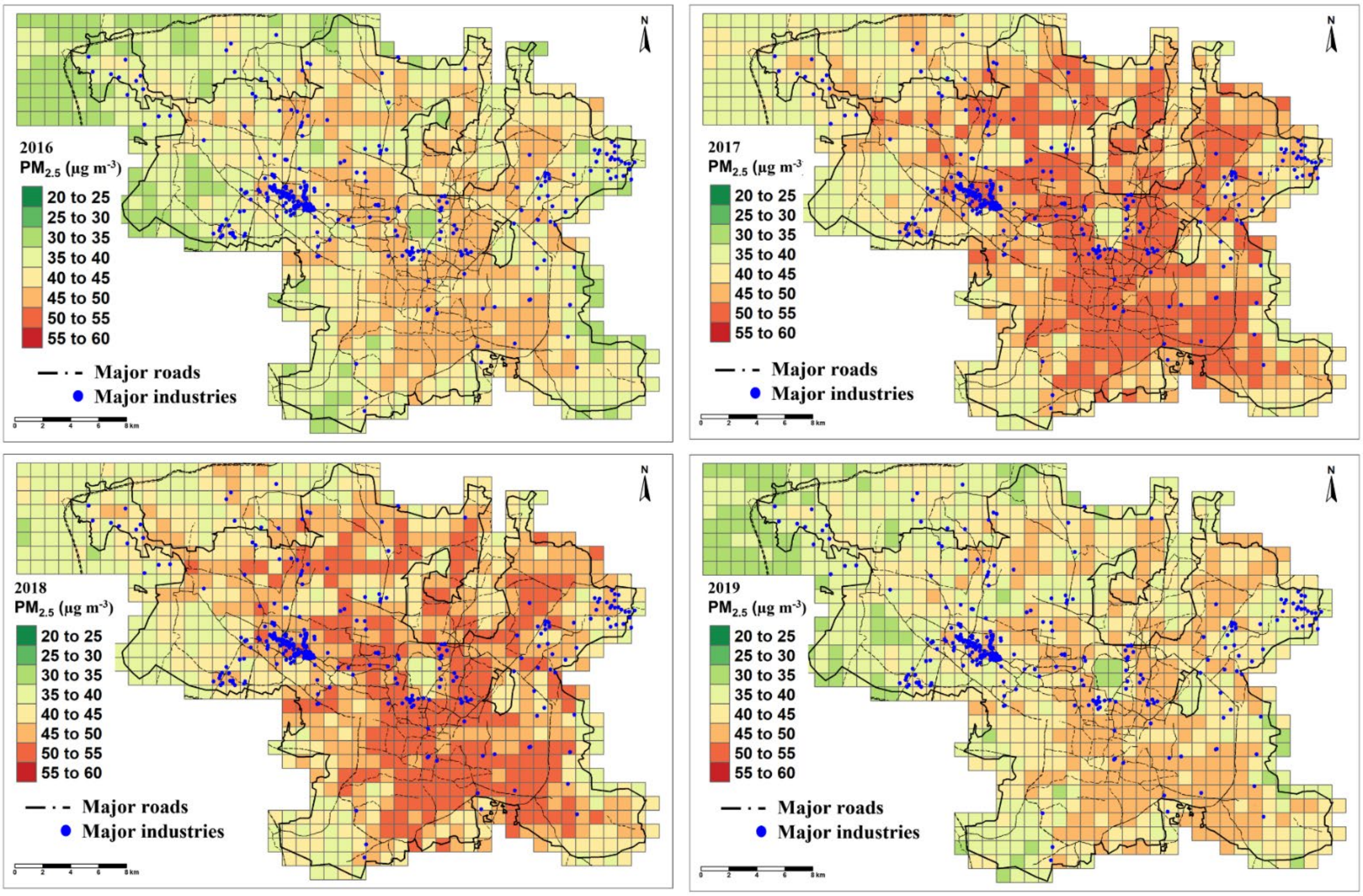

Fig. 6(b). Spatiotemporal distribution of model-derived annual average $PM_{2.5}$ concentrations in Hyderabad between 2016 and 2019.

4 CONCLUSIONS

Several PM pollution modeling studies have been conducted in India's National Capital Region (NCR) and the Indo-Gangetic plain (IGP). However, only a handful of air pollution modeling studies are published for the megacities of Bengaluru and Hyderabad with a combined population of 23 million. The population of these two cities have doubled in the last 20 years with consequent changes in land use-land cover, transportation infrastructure, etc.

In this study, the monthly-average $PM_{2.5}$ concentrations between 2016 and 2019 for 801 (1 km × 1 km) grids in Bengaluru and 873 grids in Hyderabad are derived using the LME model. The LME model shows a satisfactory performance with a ten-fold CV R^2 of 65.5% and 61.6% for Bengaluru, and Hyderabad, respectively. This paper is the first to use the LME model for the megacities of Bengaluru and Hyderabad and successfully captures the spatial and temporal variability in the $PM_{2.5}$ concentrations in both study areas. Therefore it is a valuable addition to the literature on air pollution research.

Due to the competing priorities for public finance in a developing country like India, a robust geospatial model relating ambient air pollution with remote sensing and meteorological parameters and validated with both continuous and manual AQMS data will be useful to monitor $PM_{2.5}$ pollution levels by filling up the gaps in AQMS data. Therefore, such models are particularly useful for monitoring and control of ambient air pollution in the megacities of peninsular India.

The LME models developed during this study indicate the importance of LULC changes and meteorological parameters in determining the ambient air PM concentrations in both megacities. Therefore, urban planners must take care to provide adequate green areas and public transportation (to reduce road density) as cities grow in population and size.

The grid-level $PM_{2.5}$ concentrations estimated using this research methodology can help researchers overcome the misclassification of exposure to $PM_{2.5}$ pollution in the megacities of Bengaluru and Hyderabad. As mortality and morbidity data for Indian cities are widely available every month, the $PM_{2.5}$ estimates developed with this model can be used to correlate with the monthly mortality and morbidity statistics in Bengaluru and Hyderabad. Therefore, this method is particularly suitable for exposure-response studies that must be carried out in India to assess the efficacy of India's Air Quality Standards. Ultimately, proliferation of such studies in other megacities is crucial to reduce mortality and morbidity due to air pollution-related diseases and the attainment of Sustainable Development Goals (esp. SDG 3.9).

ACKNOWLEDGMENTS

The authors are grateful to the Ministry of Earth Sciences (Grant number: MoES/16/15/2011-RDEAS (NIAS)) for supporting this research. Besides, the first author is also thankful to the Manipal Academy of Higher Education (MAHE) for permitting her to conduct her Ph.D. dissertation research entitled, 'Air Quality and Public Health: A Case Study in Bengaluru.' The authors are also grateful to Dr. Poornima Prabhakaran and Dr. Siddhartha Mandal in the Centre for Environmental Health, Prof. Diwakar, ISRO Chair Professor at NIAS, and Prof. Venugopal in the Centre for Atmospheric Sciences at the Indian Institute of Science, for their valuable guidance during this study. We also acknowledge the timely provision of data by the Central Pollution Control Board and the State Pollution Control Boards in Karnataka and Telangana without which this study would not have been possible.

REFERENCES

Ali, M.A., Assiri, M., Dambul, R. (2017). Seasonal aerosol optical depth (AOD) variability using satellite data and its comparison over Saudi Arabia for the period 2002–2013. Aerosol Air Qual Res. 17, 1267–1280. https://doi.org/10.4209/aaqr.2016.11.0492

Bangalore Development Authority (BDA) (2015). Revised Master Plan for Bengaluru-2031 (Draft). Bangalore Development Authority. https://opencity.in/pages/bda-revised-master-plan-2031-land-use-maps

Beckerman, B.S., Jerrett, M., Finkelstein, M. (2012). The association between chronic exposure to traffic-related air pollution and ischemic heart disease. J. Toxicol. Environ. Health Part A 75, 402–411. https://doi.org/10.1080/15287394.2012.670899

Beig, G., George, M.P., Sahu, S.K., Rathod, A., Singh, S., Dole, S., Murthy, B.S., Latha, R., Tikle, S., Trimbake, H.K., Shinde, R. (2020). Towards baseline air pollution under COVID-19: Implication for chronic health and policy research for Delhi, India. Curr. Sci. 119, 1178–1184. https://www.currentscience.ac.in/Volumes/119/07/1178.pdf

Beig, G., Sahu, S.K., Anand, V., Bano, S., Maji, S., Rathod, A., Korhale, N., Sobhana, S.B., Parkhi, N., Mangaraj, P., Srinivas, R., Peshin, S.K., Singh, S., Shinde, R., Trimbake, H.K. (2021). India's Maiden air quality forecasting framework for megacities of divergent environments: The SAFAR-project. Environ. Modell. Software 145, 105204. https://doi.org/10.1016/j.envsoft.2021.105204

Briggs, D.J., de Hoogh, C., Gulliver, J., Wills, J., Elliott, P., Kingham, S., Smallbone, K. (2000). A regression-based method for mapping traffic-related air pollution: Application and testing in four contrasting urban environments. Sci Total Environ. 253, 151–167. https://doi.org/10.1016/S0048-9697(00)00429-0

Center for Study of Science, Technology and Policy (CSTEP) (2022a). Source Apportionment Study for Bengaluru. (CSTEP-RR-2022-05). https://www.cstep.in/publications-details.php?id=1988

Center for Study of Science, Technology and Policy (CSTEP) (2022b). Emission inventory and pollution reduction strategies for Bengaluru. (CSTEP-RR-2022-4). https://www.cstep.in/publications-details.php?id=1985

Central Pollution Control Board (CPCB) (2013). Guidelines for the Measurement of Ambient Air Pollutants, Vol 1 and Vol 2. National Ambient Air Quality Series: NAAQMS/36/2012-13. Central Pollution Control Board, Delhi, India. https://cpcb.nic.in/openpdffile.php?id=UmVwb3J0RmlsZXMvMjdfMTQ1ODExMDQyNl9OZXdJdGVtXzE5Nl9OQUFRTVNfVm9sdW1lLUkucGRm

Chaturvedi, A. (2012). Mysore road flyover to open by sept-end. Bangalore Mirror. https://bangaloremirror.indiatimes.com/bangalore/others/mysore-road-flyover-to-open-by-sept-end/articleshow/21315949.cms

Di, Q., Kloog, I., Koutrakis, P., Lyapustin, A., Wang, Y., Schwartz, J. (2016). Assessing $PM_{2.5}$ exposures with high spatiotemporal resolution across the continental United States. Environ. Sci. Technol. 50, 4712–4721. https://doi.org/10.1021/acs.est.5b06121

Dockery, D.W., Pope, C.A., Xu, X., Spengler, J.D., Ware, J.H., Fay, M.E., Ferris, B.G., Speizer, F.E. (1993). An association between air pollution and mortality in six U.S. cities. N. Engl. J. Med. 329, 1753–1759. https://doi.org/10.1056/NEJM199312093292401

Gaigne, C., Riou, S., Thisse, J. (2010). Are Compact Cities Environmentally Friendly? GATE (Groupe D'Analyse et de Théorie Èconomique) Working Paper No. 1001. https://doi.org/10.2139/ssrn.1553776

Gałecki, A., Burzykowski, T. (2013). Linear Mixed-Effects Models Using R. Springer New York, New York, NY. https://doi.org/10.1007/978-1-4614-3900-4

Gelaro, R., McCarty, W., Suárez, M.J., Todling, R., Molod, A., Takacs, L., Randles, C.A., Darmenov, A., Bosilovich, M.G., Reichle, R., Wargan, K., Coy, L., Cullather, R., Draper, C., Akella, S., Buchard, V., Conaty, A., da Silva, A.M., Gu, W., Kim, G.K., *et al.* (2017). The Modern-Era Retrospective analysis for Research and Applications, Version 2 (MERRA-2). J. Clim. 30, 5419–5454. https://doi.org/10.1175/JCLI-D-16-0758.1

Gilbert, N.L., Goldberg, M.S., Beckerman, B., Brook, J.R., Jerrett, M. (2005). Assessing spatial variability of ambient nitrogen dioxide in Montreal, Canada, with a land-use regression model. J. Air Waste Manage. Assoc. 55, 1059–1063. https://doi.org/10.1080/10473289.2005.10464708

Gorelick, N., Hancher, M., Dixon, M., Ilyushchenko, S., Thau, D., Moore, R. (2017). Google Earth Engine: Planetary-scale geospatial analysis for everyone. Remote Sens. Environ. 202, 18–27. https://doi.org/10.1016/j.rse.2017.06.031

Gupta, A., Kant, Y., Mitra, D., Chauhan, P. (2020). Spatio-temporal distribution of INSAT-3D AOD derived particulate matter concentration over India. Atmos. Pollut. Res. 12, 159–172. https://doi.org/10.1016/j.apr.2020.08.031

Guttikunda, S.K., Nishadh, K.A., Gota, S., Singh, P., Chanda, A., Jawahar, P., Asundi, J. (2019). Air quality, emissions, and source contributions analysis for the Greater Bengaluru region of India. Atmos. Pollut. Res. 10, 941–953. https://doi.org/10.1016/j.apr.2019.01.002

Health Effects Institute (2020). State of Global Air 2020. Special Report. Health Effects Institute, Boston.

Indian Meteorological Department (IMD) (2010–2020). https://dsp.imdpune.gov.in/

Jerrett, M., Burnett, R.T., Ma, R. (2005). Spatial analysis of air pollution and mortality in Los Angeles. Epidemiology 16, 727–736. https://doi.org/10.1097/01.ede.0000181630.15826.7d

Jerrett, M., Burnett, R.T., Pope, C.A., Ito, K., Thurston, G., Krewski, D., Shi, Y., Calle, E., Thun, M. (2009). Long-term ozone exposure and mortality. N. Engl. J. Med. 360, 1085–1095. https://doi.org/10.1056/NEJMoa0803894

Just, A.C., Wright, R.O., Schwartz, J., Coull, B.A., Baccarelli, A.A., Tellez-Rojo, M.M., Moody, E., Wang, Y., Lyapustin, A., Kloog, I. (2015). Using high-resolution satellite aerosol optical depth to estimate daily $PM_{2.5}$ geographical distribution in Mexico city. Environ. Sci. Technol. 49, 8576–8584. https://doi.org/10.1021/acs.est.5b00859

Kim, S.Y., Sheppard, L., Kim, H. (2009). Health effects of long-term air pollution: Influence of exposure prediction methods. Epidemiology 20, 442–450. https://doi.org/10.1097/EDE.0b013e31819e4331

Kloog, I., Koutrakis, P., Coull, B.A., Lee, H.J., Schwartz, J. (2011). Assessing temporally and spatially resolved $PM_{2.5}$ exposures for epidemiological studies using satellite aerosol optical depth measurements. Atmos. Environ. 45, 6267–6275. https://doi.org/10.1016/j.atmosenv.2011.08.066

Kloog, I., Chudnovsky, A.A., Just, A.C., Nordio, F., Koutrakis, P., Coull, B.A., Lyapustin, A., Wang, Y., Schwartz, J. (2014). A new hybrid spatio-temporal model for estimating daily multi-year $PM_{2.5}$ concentrations across northeastern USA using high resolution aerosol optical depth data. Atmos. Environ. 95, 581–590. https://doi.org/10.1016/j.atmosenv.2014.07.014

Krewski, D., Burnett, R.T., Goldberg, M., Hoover, K., Siemiatycki, J., Abrahamowicz, M., Villeneuve, P.J., White, W. (2005). Reanalysis of the harvard six cities study, Part II: Sensitivity analysis. Inhalation Toxicol. 17, 343–353. https://doi.org/10.1080/08958370590929439

Kutner, M.H., Nachtsheim, C.J., Neter, J. (1983). Applied Linear Regression Models. 4th Edition. McGraw-Hill Irwin Publication. New York.
Lavanyaa, V.P., Srikanth, R. (2020). Air quality in Bengaluru improves significantly post the lockdown. https://www.thehindubusinessline.com/opinion/air-quality-in-bengaluru-improves-significantly-post-the-lockdown/article31516048.ece
Lloyd, S.P. (1982). Least squares quantification in PCM. IEEE Trans. Inf. Theory 28, 129–137. https://doi.org/10.1109/TIT.1982.1056489
Lyapustin, A., Wang, Y., Korkin, S., Huang, D. (2018). MODIS collection 6 MAIAC algorithm. Atmos. Meas. Tech. 11, 5741–5765. https://doi.org/10.5194/amt-11-5741-2018
Macrotrends (2022). https://www.macrotrends.net/countries/IND/india/population
Maheshwarkar, P., Sunder Raman, R. (2021). Population exposure across central India to $PM_{2.5}$ derived using remotely sensed products in a three-stage statistical model. Sci. Rep. 11, 544. https://doi.org/10.1038/s41598-020-79229-7
Mandal, S., Madhipatla, K.K., Guttikunda, S., Kloog, I., Prabhakaran, D., Schwartz, J.D. (2020). Ensemble averaging based assessment of spatiotemporal variations in ambient $PM_{2.5}$ concentrations over Delhi, India, during 2010–2016. Atmos Environ. 224, 117309. https://doi.org/10.1016/j.atmosenv.2020.117309
Miller, K.A., Siscovick, D.S., Sheppard, L., Shepherd, K., Sullivan, J.H., Anderson, G.L., Kaufman, J.D. (2007). Long-Term Exposure to Air Pollution and Incidence of Cardiovascular Events in Women. N. Engl. J. Med. 356, 447–458. https://doi.org/10.1056/NEJMoa054409
Ministry of Environment, Forest and Climate Change (MoEFCC) (2020a). Continuous ambient air quality monitoring stations. Reply given by Hon Minister of Environment, Forest and Climate Change to question no. 4514 in the Lok Sabha on 20 March, 2020. http://164.100.24.220/loksabhaquestions/annex/173/AU4514.pdf
Ministry of Environment, Forest and Climate Change (MoEFCC) (2020b). Most polluted cities. Reply given by Hon Minister of Environment, Forest and Climate Change to question no. 973 in the Lok Sabha on 18 September, 2020. http://164.100.24.220/loksabhaquestions/annex/174/AU973.pdf
Mondal, A., Sharma, S.K., Mandal, T.K., Girach, I., Ojha, N. (2021). Frequency distribution of pollutant concentrations over Indian megacities impacted by the COVID-19 lockdown. Environ. Sci. Pollut. Res. https://doi.org/10.1007/s11356-021-16874-z
Monn, C. (2001). Exposure assessment of air pollutants: a review on spatial heterogeneity and indoor/outdoor/personal exposure to suspended particulate matter, nitrogen dioxide and ozone. Atmos Environ. 35, 1–32. https://doi.org/10.1016/S1352-2310(00)00330-7
Mukherjee, S. (2012). Whitefield is the most polluted area in Bangalore. https://timesofindia.indiatimes.com/city/bengaluru/Whitefield-is-most-polluted-area-in-Bangalore/articleshow/12000809.cms
National Green Tribunal (NGT) (2021). Hearing on Original Application No. 681/2018, (With reports dated 05.04.2021 and 05.02.2021), Item No. 05. https://greentribunal.gov.in/gen_pdf_test.php?filepath=L25ndF9kb2N1bWVudHMvbmd0L2Nhc2Vkb2MvanVkZ2VtZW50cy9ERUxISS8yMDIxLTA0LTA4LzE2MTgzODgzNjkxNjI3OTgyMzU2MDc2YTU5MTdjNWQ1LnBkZg==
National Oceanic and Atmospheric Administration (NOAA) (2012). GOES-R Advanced Baseline Imager (ABI) Algorithm Theoretical Basis Document for Suspended Matter/Aerosol Optical Depth and Aerosol Size Parameter. https://www.star.nesdis.noaa.gov/goesr/docs/ATBD/AOD.pdf
Ojha, N., Sharma, A., Kumar, M., Girach, I., Ansari, T.U., Sharma, S.K., Singh, N., Pozzer, A., Gunthe, S.S. (2020). On the widespread enhancement in fine particulate matter across the Indo-Gangetic Plain towards winter. Sci. Rep. 10, 5862. https://doi.org/10.1038/s41598-020-62710-8
OpenStreetMap (2021). https://www.openstreetmap.org/#map=11/17.4325/78.4293
Özkaynak, H., Baxter, L.K., Dionisio, K.L., Burke, J. (2013). Air pollution exposure prediction approaches used in air pollution epidemiology studies. J. Exposure Sci. Environ. Epidemiol. 23, 566–572. https://doi.org/10.1038/jes.2013.15
Pope III, C.A., Burnett, R.T., Thun, M.J., Calle, E.E., Krewski, D., Ito, K., Thurston, G.D. (2002). Lung cancer, cardiopulmonary mortality, and long-term exposure to fine particulate air pollution. JAMA 287, 1132–1141. https://doi.org/10.1001/jama.287.9.1132
Pope III, C.A., Ezzati, M., Dockery, D.W. (2009). Fine-particulate air pollution and life expectancy

in the United States. N. Engl. J. Med. 360, 376–386. https://doi.org/10.1056/NEJMsa0805646

Prabhakaran, P., Jaganathan, S., Walia, G.K., Wellenius, G.A., Mandal, S., Kumar, K., Kloog, I., Lane, K., Nori-Sarma, A., Rosenqvist, M., Dahlquist, M., Reddy, K.S., Schwartz, J., Prabhakaran, D., Ljungman, P.L.S. (2020). Building capacity for air pollution epidemiology in India. Environ. Epidemiol. 4, e117. https://doi.org/10.1097/EE9.0000000000000117

QGIS Documentation (2021). A Gentle Introduction to Q GIS. https://docs.qgis.org/3.16/en/docs/gentle_gis_introduction/index.html

Randles, C.A., da Silva, A.M., Buchard, V., Colarco, P.R., Darmenov, A., Govindaraju, R., Smirnov, A., Holben, B., Ferrare, R., Hair, J., Shinozuka, Y., Flynn, C.J. (2017). The MERRA-2 aerosol reanalysis, 1980 onward. Part I: System description and data assimilation evaluation. J. Clim. 30, 6823–6850. https://doi.org/10.1175/JCLI-D-16-0609.1

Rani, S.I., T, A., George, J.P., Rajagopal, E.N., Renshaw, R., Maycock, A., Barker, D.M., Rajeevan, M. (2021). IMDAA: High resolution satellite-era reanalysis for the indian monsoon region. J. Clim. 1–78. https://doi.org/10.1175/JCLI-D-20-0412.1

Ross, Z., English, P.B., Scalf, R., Gunier, R., Smorodinsky, S., Wall, S., Jerrett, M. (2006). Nitrogen dioxide prediction in Southern California using land use regression modeling: Potential for environmental health analyses. J. Exposure Sci. Environ. Epidemiol. 16, 106–114. https://doi.org/10.1038/sj.jea.7500442

Salam, M.T., Millstein, J., Li, Y.F., Lurmann, F.W., Margolis, H.G., Gilliland, F.D. (2005). Birth outcomes and prenatal exposure to ozone, carbon monoxide, and particulate matter: Results from the children's health study. Environ. Health Perspect. 113, 1638–1644. https://doi.org/10.1289/ehp.8111

Samet, J.M., Dominici, F., Curriero, F.C., Coursac, I., Zeger, S.L. (2000). Fine particulate air pollution and mortality in 20 U.S. Cities, 1987–1994. N. Engl. J. Med. 343, 1742–1749. https://doi.org/10.1056/NEJM200012143432401

Sanchez, M., Ambros, A., Milà, C., Salmon, M., Balakrishnan, K., Sambandam, S., Sreekanth, V., Marshall, J.D., Tonne, C. (2018). Development of land-use regression models for fine particles and black carbon in peri-urban South India. Sci. Total Environ. 634, 77–86. https://doi.org/10.1016/j.scitotenv.2018.03.308

Sarrat, C., Lemonsu, A., Masson, V., Guedalia, D. (2006). Impact of urban heat island on regional atmospheric pollution. Atmos. Environ. 40, 1743–1758. https://doi.org/10.1016/j.atmosenv.2005.11.037

Sastry, A.K. (2012). Work on a two-level BDA flyover in Mysore Road crawls. https://www.thehindu.com/news/cities/bangalore/work-on-twolevel-bda-flyover-on-mysore-road-crawls/article3295978.ece

Shy, C.M., Kleinbaum, D.G., Morgenstern, H. (1978). The effects of misclassification of exposure status in epidemiological studies of air pollution health effects. Bull. N. Y. Acad. Med. 54, 1155–1165.

Singh, V., Singh, S., Biswal, A., Kesarkar, A.P., Mor, S., Ravindra, K. (2020). Diurnal and temporal changes in air pollution during COVID-19 strict lockdown over different regions of India. Environ Pollut. 266, 115368. https://doi.org/10.1016/j.envpol.2020.115368

Stafoggia, M., Schwartz, J., Badaloni, C., Bellander, T., Alessandrini, E., Cattani, G., de' Donato, F., Gaeta, A., Leone, G., Lyapustin, A., Sorek-Hamer, M., de Hoogh, K., Di, Q., Forastiere, F., Kloog, I. (2017). Estimation of daily PM_{10} concentrations in Italy (2006–2012) using finely resolved satellite data, land use variables and meteorology. Environ. Int. 99, 234–244. https://doi.org/10.1016/j.envint.2016.11.024

Stedman, J.R., Vincent, K.J., Campbell, G.W., Goodwin, J.W.L., Downing, C.E.H. (1997). New high resolution maps of estimated background ambient NO_x and NO_2 concentrations in the U.K. Atmos. Environ. 31, 3591–3602. https://doi.org/10.1016/S1352-2310(97)00159-3

Stone, M. (1974). Cross-validatory choice and assessment of statistical predictions. J. R. Stat. Soc. B 36, 111–147. https://doi.org/10.1111/j.2517-6161.1974.tb00994.x

Sun, L., Li, R.B., Tian, X.P., Wei, J. (2017). Analysis of the temporal and spatial variation of aerosols in the Beijing-Tianjin-Hebei region with a 1 km AOD product. Aerosol Air Qual. Res. 17, 923–935. https://doi.org/10.4209/aaqr.2016.05.0185

The Hindu (2019). Graphite India shuts shop in Bengaluru. https://www.thehindu.com/news/cities/bangalore/its-official-graphite-india-shuts-shop-in-bengaluru/article26725043.ece

The New Indian Express (2017). All of Bangalore Metro Phase-1 will be up and running from 18 June. https://www.newindianexpress.com/cities/bengaluru/2017/jun/08/all-of-bangalore-metro-phase-1-will-be-up-and-running-from-june-18-1614155.html